This is a repository copy of *Plasma additive layer manufacture smoothing (PALMS) technology – An industrial prototype machine development and a comparative study on both additive manufactured and conventional machined AISI 316 stainless steel*.

White Rose Research Online URL for this paper:
https://eprints.whiterose.ac.uk/160062/

Version: Accepted Version

Article:

Yang, L orcid.org/0000-0003-0935-3921, Laugel, N, Housden, J et al. (3 more authors) (2020) Plasma additive layer manufacture smoothing (PALMS) technology – An industrial prototype machine development and a comparative study on both additive manufactured and conventional machined AISI 316 stainless steel. Additive Manufacturing, 34. 101204. ISSN 2214-7810

https://doi.org/10.1016/j.addma.2020.101204

Plasma Additive Layer Manufacture Smoothing (PALMS) Technology – An

Industrial Prototype Machine Development and a Comparative Study on Both

Additive Manufactured and Conventional Machined AISI 316 Stainless Steel

Liuquan Yang[a]*, Nicolas Laugel[b], Jonathan Housden[a], Laurent Espitalier[a],

Allan Matthews[b] and Aleksey Yerokhin[b]

[a] Wallwork Cambridge Limited, Buckingway Business Park, Swavesey, Cambridge, CB24 4UG, UK

[b] School of Materials, The University of Manchester, Manchester, M13 9PL, UK

* Corresponding author: Tel: +44 (0)1954 233700. E-mail:

liuquan.yang@wallworkht.com (now at University of Leeds,

l.q.yang@leeds.ac.uk).

Plasma Additive Layer Manufacture Smoothing (PALMS) Technology – An Industrial Prototype Machine Development and a Comparative Study on Both Additive Manufactured and Conventional Machined AISI 316 Stainless Steel

L. Yang[a*], N. Laugel[b], J. Housden[a], L. Espitalier[a], A. Matthews[b] and A. Yerokhin[b]

[a] Wallwork Cambridge Limited, Buckingway Business Park, Swavesey, Cambridge, CB24 4UG, UK

[b] School of Materials, The University of Manchester, Manchester, M13 9PL, UK

Abstract

Additive Layer Manufacturing (ALM) of metals is rapidly changing the landscape of industrial manufacturing. Its deployment is however still hindered by extremely rough native surfaces, and drastic difficulties in efficiently applying conventional finishing methods. This paper presents the PALMS process, derived from electrolytic plasma polishing, as a solution to this problem. The viability of the process on a scale compatible with commercial use is demonstrated with a prototype industrial implementation. PALMS was applied on AISI 316 stainless steel pieces produced either by ALM or by conventional machining (CM.) Surface states, microstructures and other properties were compared pre- and post-PALMS. Significant improvements in surface state were observed after a 10 minutes treatment, with a 5-fold reduction in roughness. ALM surfaces were not affected negatively by PALMS in any way measured, and showed slight improvements in hardness and pore density. Two PVD coatings (TiN and

* Corresponding author.
Tel.: +44 (0) 1954 233700
E-mail address: liuquan.yang@wallworkht.com (now at University of Leeds, l.q.yang@leeds.ac.uk)

WCC) were finally applied Post-PALMS, to test the compatibility of the process with further industrially relevant surface treatments. PALMS enables good coating adhesion on ALM pieces, with improved friction and wear properties compared to their CM counterparts.

1. Introduction

Metal additive manufacturing (AM) or additive layer manufacturing (ALM) has been researched and developed over the last three decades in conjunction with advancements in material science, computer aided design and automation [1-7]. The scientific research and engineering has been focused on high value sectors such as aerospace, automotive, medical (dental, implants) and electronic applications [3, 6]. Whilst a more fundamental focus has been put on the metallurgical design of alloys, and on the development of printing equipment, modelling techniques and laser/electron-beam [6-8], most of the engineering challenges centre around dimensions precision, printing speed, component size, complex structure, etc. Among those challenges, the surfaces of ALM parts often exhibit a layered structure perpendicular to the build direction with granulated facets, resulting from the fused granular feed-stock. Moreover, a rough surface at the length scales associated with the discretization (numerical CAD/print resolution, particle size of the feed powder) is typical [7]. Additional chemical and/or mechanical finishing methods have been introduced to address this challenge as post-printing procedures [2-4, 7], depending on the precision required on piece dimensions and surface finish as well as on the nature of the material to be processed. Where high precision finishes are required, conventional machining methods such as micro machining process (MMP) can be time consuming and are not effective in finishing complex internal structures. Another important consideration is the fact that the current quality systems as defined in ISO are not developed for freeform shapes and associated tolerances [7].

Mechanical properties, microstructure and material chemistry of AM materials and the conventional wrought materials differ [5, 9]. Also, additional complexities arise in

the challenge of smoothing the ALM surfaces, with as yet poorly understood surface science and much research still to be addressed. This study focuses on the Plasma Additive Layer Manufacturing Smoothing (PALMS) technology, an innovative bespoke designed process derived from electrolytic plasma polishing (EPPo)[10-14]. The method is applied on the treating of one of the most commonly ALM printed materials, AISI 316 stainless steel. The conventional EPPo process may face some new challenges and unknowns when brought to the ALM industry, as it is typically applied on traditionally manufactured components either for highly reflective mirror finishing and deburring, or removal of rusty oxide or other undesired surface-bound species. However, due to the nature of the method and in particular the creation of temporary supporting structures, ALM typically involves a large amount of subtractive manufacturing as a finishing step[15]. Even so, ALM still achieves great material utilization compared to conventional subtractive manufacturing, *e.g.* a wrought process followed by machining off large amounts of the original material. Some work on electrochemical machining (ECM) for polishing ALM manufactured Inconel 718 was also researched [16] in the context of surface improvement. Conventional polishing methods, either ECM or conventional EPPo, typically result in retention of the existing topographic features of the components, leading to difficulties in meeting the desired precision of ALM printed components [11, 15, 16]. Additionally, ECM is time/energy consuming and the electrolytes used are subject to stringent REACh regulations [17]; whereas EPPo (including PALMS) based methods use low concentration salts in an aqueous solution with pH = 5-7 [11, 12].

A first industrial based prototype PALMS machine was built in order to study the science and engineering aspects of treating ALM printed 316 stainless steel (AISI 316)

samples in comparison to conventionally manufactured and machined AISI 316. The PALMS machine and process was specifically designed to address the complexity of the additive manufactured components and to enable a study of the science aspects. Studies of the process effectiveness and surface characterisation have been carried out. PALMS technology has been shown to improve the surface finishing and satisfy the proposed targets with a 10 minute treatment time. The AISI 316 surface was also slightly hardened after PALMS process following the EPPo principle. Different surface patterns have been observed between ALM and conventionally machined materials. The superior smoothing of surfaces by the PALMS treatment indicated the promising potential of the modified EPPo technology in providing for the first time a cost effective and environmentally friendly finishing process for the metal 3D printing industry. Research into PALMS science and engineering is highlighting a number of unknowns that EPPo principle has yet to be conducted comprehensively due to the nature of additive manufacturing. However, it opens the door for the use of EPPo principle (PALMS technology) for additive manufacturing.

2. PALMS Technology – Industrial Prototype Machine Development

2.1 Principle of Electrolytic Plasma Polishing – Origin of the PALMS Technology

The use of plasma electrolysis principles in surface science has been broadly applied in terms of plasma electrolytic oxidation, deposition, saturation, and cleaning, as well as polishing in order to improve the surface properties [13]. Achieving a high precision metal surface finish would lead to electrolytic plasma polishing (EPPo) becoming one of the promising candidates, since it offers both polishing efficiency and meets surface

quality targets as well as addressing environmental concerns [11]. Research into EPPo has been carried out in the past in terms of controlling material removal rate, process optimisation, uniformity of the process, scale up of the process, extending the candidate alloys to be polished, and the scientific understanding of such a mechano-electrochemical process [11-13, 18]. The basic principle of any EPPo process is an anodic process which involves the use of a relatively high voltage (ca. 250 to 500 V) power supply connected to the work piece to be polished. The process is typically carried out in low concentration, environmental friendly aqueous salt solutions. When the work piece is immersed in the solution at a certain current density, conventional electrolysis is interrupted by the formation of a gaseous phase which follows the classical electrochemistry but at high voltage. The gas envelope separates the working electrode surface from the electrolyte completely in a dynamic way which consists of nucleation, growth and detachment of gas bubbles from the electrode surface due to both surface tension and buoyancy forces as suggested by Vogt [19]. During such a process, the anodic surface being treated is exposed to pulsed electrical discharges on the surface asperities and dynamic contacts of chemically active medium which lead to material removal and polishing.

Due to the nature of the process, most of the current research starts with surface roughness $S_a < 1$ µm and finishes the metal surface down to $S_a < 0.02$ µm [11, 18] for different metal alloys. It generally considers an overall material removal of the workpiece. Therefore, conventional processes following EPPo principle is effective for polishing but not applicable to rougher surfaces as some of the undesired, larger surface topographical features may be retained in a short process time [11] unless a longer process time is implemented. There is a gap in the research for rougher surfaces with

challenges such as process control, current density variation and material removal/geometry precision which PALMS technology addressed in this study. These challenges align well with ALM printed components with a rough finish (typically 0.5 µm < S_a < 50 µm). The answer to finishing rough and complex geometry ALM components is not simply a longer treatment time based on traditional EPPo process. Also the target to be achieved for ALM surface finishing is not simply a mirror finish. It has been shown that EPPo polishing would normally result in a continuous reduction in mechanical hardness on the surface as a function of polishing time [18]. To maintain the mechanical strength of ALM components is essential for high value manufactured components. A large amount of material removal from a rough surface by the traditional EPPo process may generate considerable volumes of floc in the electrolyte which could disrupt the process.

2.2 PALMS Industrial Prototype Machine Design and Configuration

An industrial prototype PALMS machine was built in house (Fig. 1), designed to incorporate the differences required from the traditional EPPo process in order to address the challenges in ALM surfaces. It featured circulation, settling and temperature control systems, as well as workpiece loading control. A 30 kW power supply was used based on the surface areas of components to be treated. Comprehensive means of electrical conductivity and pH monitoring were incorporated in the design. The overall process is closely controlled, enabling studies on complex ALM components. A strong and stable plasma electrical discharge on one of the large tested pieces is demonstrated in Fig. 2.

8

2.3 Challenges in ALM Surface Finishing and the Benefit of PALMS Technology

The post processing of ALM components would normally be addressed on a case by case basis due to a number of complicating variables including materials, printing technologies, geometries, different heat treatment methods, etc [2-5, 7, 15, 20]. Therefore, the current state of the art research has been primarily aimed at utilising existing techniques which are summarized in Table 1. It should be noted that these comments were summarised based on ALM components with small and complex geometrical details that would be either too time consuming (hence cost-prohibitive) or impossible to handle by conventional mechanical machining.

3. Experimental Methods

3.1 Materials and Sample Preparation

CM and ALM test pieces made of AISI 316 were chosen. CM test discs (⌀ 25 mm x 3 mm) were used as the reference and were uniformly mechanically roughened by grit blasting, giving all the CM reference test pieces a similar level of surface roughness. ALM test discs (⌀ 30 mm x 3 mm) printed by 3T RPD® using an industrial scale printer based on Direct Metal Laser Sintering (DMLS), a representative powder bed based printing method, were studied and compared with the CM material. The printer was an EOSINT M290 metal sintering machine with the effective building volume (including building platform) of 250mm x 250mm x 325mm. The 400W power Yb-fibre laser was used with typical build speed 2-8 mm^3/s. The layer thickness was 40 µm. Because glass bead abrasive blasting is a standard post-printing initial finishing procedure frequently employed by printing bureaus, the ALM discs were supplied blasted. Dry-grit blasting

of the CM test discs produced a surface finish approximating to that of the as-supplied ALM discs thereby enabling valid comparisons. All the samples were cleaned in an industrial aqueous ultrasonic cleaning line and weighed. The surface parameters, chemical and mechanical properties were all measured both pre- and Post-PALMS treatment and compared for both types of test samples. The ALM samples satisfied the manufacturer's ISO9001:2008 quality assurance. They were usually greater than 99 % dense which required no further sintering or other infiltration process to achieve full density. No heat treatment or any other stress-relieving procedure were applied on the samples used in this work.

3.2 PALMS Technology Experiments

The environmentally friendly electrolyte (pH = 5-7) with 4-8 wt% salt concentration was blended in the circulating system of the prototype machine shown in Fig. 1. In order to establish the effects of PALMS process treatment time on ALM AISI 316, one ALM test disc was PALMS-treated for 90 minutes in 10 minute steps with topographic and gravimetric measurements carried out after each step. Referring to an aerospace surface finish specification [21], the PALMS process could achieve such specification within the first ten minutes. The subsequent comparative studies of ALM and CM AISI 316 were then carried out using a fixed process time of 10 minutes. The process voltage was 350 V and the process temperature was between 60-90 ℃. The electrolyte temperature, pH and conductivity, as well as the current density were monitored during the process. The test discs were cleaned again after PALMS treatment in the ultrasonic cleaning line and then stored in a desiccator for further analyses.

3.3 Material and Surface Characterisations

  Surface parameters, tribological wear measurements and particle/porosity analyses were evaluated by non-contact 3D optical surface profilometry based on light interference using a Zemetrics ZeScope model. Prior to the measurements, the test samples were rinsed in water, cleaned by Isopropyl alcohol and dried in air before and after the treatment. Data collected were from 3 independent experiments for each material. Surface parameters, S_a (roughness), S_q (root mean square roughness), S_z (average distance of peak to trough) were derived from the recorded height maps (449 µm x 335 µm). A Carl Zeiss EVO MA25 SEM equipped with an EDS system was employed for the morphological and chemical analyses with secondary electron mode at 20 kV. A Zeiss M1M optical microscope was used for optical analyses on both the surface and cross-sectional layered structure on the ALM samples. A Mitutoyo 810-129E microhardness tester equipped with Vickers indenter was employed on both surface microhardness (at 2 kgf) and cross-sectional microhardness (at 0.5 kgf), respectively. Instrumented indentation by Fisherscope HM2000-XYp equipment (load-indentation depth method) was employed for a depth profile of the hardness on the cross section of the PALMS treated samples starting from the edge of the surface. X ray diffraction (XRD) was performed on a Bruker D8 Discover (Cu radiation, $\lambda = 1.54$ Å). Peak analysis was performed using the Highscore Plus software. The results reported, in particular concerning peak widths and areas, were confirmed to be independent of sample alignment through measurements varying the in-plane sample orientation (Phi). DS (divergence-limiting slits) of 0.2 and 0.6 mm were used in experimental repetitions, to further confirm the absence of sample positioning artefacts affecting the results.

3.4 Coatings Sample Preparation and Related Tribological Testing

As a metal smoothing process, the quality of the PALMS surface finish and its tribological performance were investigated. The assessment of PALMS technology and conventional machining/polishing was essential to demonstrate the viability of such a process. Two Wallwork Cambridge commercial PVD coatings, Titanium nitride (TiN) and tungsten carbide-carbon (WCC) were deposited using TECVAC industrial coating equipment built in-house on both the PALMS treated and conventionally lapped/polished test discs. These coated samples were then evaluated in terms of friction, wear, load carrying capacity, adhesion, and mechanical properties. A CSM Instruments Revetest scratch tester was employed for scratch adhesion and load carrying capacity evaluation of coated samples (with diamond indenter) as well as friction coefficient measurement at ambient conditions (Relative Humidity 44.8 %, Temperature 20.4 ℃, 10 m reciprocating distance for 18 minutes, 10 N load, tungsten carbide ball with diameter 6 mm). Coating adhesion was also assessed by Rockwell C indentation. The tribotests were performed using a tungsten carbide ball against the coated test discs in a non-lubricated environment. The wear scars of the coated surfaces after the tribotest were measured and the wear rates were calculated as described elsewhere [22].

4. Results and Discussions

4.1 Effectiveness of PALMS on ALM AISI 316 Stainless Steel – Process Time vs. Surface Roughness Parameters

Firstly the process time required achieving an acceptable level of surface finish by PALMS, comparable to that achieved by conventional machining was studied. The primary target was set to $S_a < 0.8$ µm together with a reduction in S_z as was required by an aerospace specification [21]. The focus of the study was not polishing but smoothing the rough finished ALM 3D printed components. One ALM test disc with the standard glass bead blasting finish was experimentally processed for 90 minutes, in 10 minute steps with the sample removed for measurements after each step (Fig. 3). After 10 minute PALMS process, the ALM test disc achieved $S_a = 0.6$ µm (down from 3.0 µm), $S_q = 0.7$ µm (down from 3.6µm) and $S_z = 4.0$ µm (down from 23.9 µm). It should also be noted that at least 3 different positions were generally surveyed and averaged to provide a good representation on the surface finish of the ALM test discs. The 10 minute process also resulted in an optically reflective surface on the ALM disc (originally matt) as shown in photographs Fig. 4. Confirming visual inspection, the surface glossiness at a 60° incident angle increased dramatically after treatment. Glossiness units (GU) were calibrated against a reflective but dark reference, whose glossiness is set at 100. Pre-PALMS CM samples average at 2.0 GU, while their Post-PALMS counterparts reach the saturation value for the glossmeter and conditions used, 240 GU. ALM downskin surfaces similarly went from 13.5 Pre-PALMS to 240 GU Post-PALMS, and the rougher ALM upskin surfaces from 10.0 to 150 GU. Despite direct reflection of light sources on the photograph perhaps suggesting a smoother surface, the curved sides of ALM samples (Fig. 4, bottom panels) display surfaces very similar visually to their downskin counterparts. Additional work has been conducted specifically on curved and inner surfaces, and will be covered in a subsequent publication. At the end of the 90 minute process, surface parameters reached $S_a = 0.1$

µm, S_q = 0.2 µm and S_z = 1.8 µm, respectively. As the target S_a was achieved within the first 10 minutes processing time, the comparative study in this paper was carried out using a 10 minute PALMS treatment. Other effects of the PALMS process on the ALM components were not investigated and so are still largely unknown especially on complex geometry parts and will be studied in follow up projects. Visual inspection of the 10 minute PALMS treated CM and ALM samples indicated the reflective surface quality improved on both CM and ALM AISI 316 test discs (Fig. 4). The CM AISI 316 discs were mechanically roughened by grit blasting (matt) prior to PALMS treatment. Detailed comparisons of the two materials both pre-and Post-PALMS treatment are discussed in Section 4.3.

4.2 Effect of PALMS on the Tribological Performance of Coated Components on AISI 316 Stainless Steel Substrates

The coefficient of friction maintained similar levels for both PALMS and non-PALMS treated lapped and polished AISI 316 surfaces when TiN and WCC coated, respectively (Fig. 5) even though the actual surface of the lapped and polished discs was much smoother (S_a = 0.1 µm) than the PALMS treated surfaces (S_a = 0.6 µm, Table 2). Coatings deposited on PALMS treated samples showed over 10 % reduction in friction coefficient (Fig. 5), in line with the observed wear rates (both wear coefficient and maximum depth of wear scar). These wear results are shown in Table 2 together with scratch adhesion data which show coating adhesion levels in the PALMS sample were maintained compared to the standard lapped and polished, coated sample. The present study was primarily aimed at verifying the substrate properties and the effect of PALMS. However, it is worth noting that the formation of a dimpled surface texture by the

14

PALMS/EPPo process (discussed in the later SEM surface analyses) might be contributing to the reduction in friction and wear. WCC carbon based coating showed a smaller reduction in friction and wear compared with the TiN coated surface which was thought to be due to the self-lubricating properties of the carbon based coating commonly reported in literature [22]. For thin film coating by a vacuum deposition process, surface preparation is critical to maintain good adhesion for good coating quality and good tribological performance. PALMS treated samples, subsequently PVD coated, can therefore achieve the same high level of tribological performance as the conventionally lapped and polished surfaces with the same coating (Table 2). Initial tribotesting results therefore bring some confidence in the validity of the PALMS technology for applications where moving surfaces are in direct contact and wear would occur due to larger asperities.

4.3 PALMS Comparative Study of Conventional Manufactured and ALM Printed AISI 316 Stainless Steel

4.3.1 The Surface Finish Assessments

The effect of the PALMS process on the surface parameters of CM and ALM AISI 316 is shown in Fig. 6 and Fig. 7, respectively. The surface parameters S_a, S_q and S_z are widely used in tribology publications, and have therefore been measured and are presented below. For both CM and ALM test discs, at the measured length scale, PALMS technology was shown to significantly improve the surface roughness S_a and S_q, to similar levels. Whilst ALM samples were actually rougher than the mechanically roughened CM samples before treatment, the improvement in S_z was more pronounced in the ALM than the CM samples. Such an improvement would suggest a potential

improvement in tribological performance particularly in the frictional motions on contact asperities (Fig. 5). The differences in surface roughness are further considered in relation to the chemical and microstructure characteristics described in the next few sections. The standard deviations of S_a and S_q, calculated from three measurements made on each of two test discs, were relatively small, showing that the PALMS process, at this one set of experimental conditions, reliably produces homogeneous surface finishing for both CM and ALM materials.

4.3.2 Gravimetric Study and Change in Current Density Related to Sample Geometry

A gravimetric study was carried out by weighing three individual test discs pre- and Post-PALMS process for both ALM and CM, respectively. Surface areas based on the known geometry were calculated for these test pieces and the changes in current density during the 10 minute process were both summarised in Table 3. The mass loss for both CM and ALM was less than 2 wt% whilst ALM has slightly more mass loss compared with CM. It was observed that the average S_z of the Post-PALMS ALM samples was much smaller than that of the CM samples whilst both started at similar level, Pre-PALMS treatment (Figs. 6 and 7). Therefore, the PALMS process appeared to have improved the surface finish by removing more material from the ALM samples during the smoothing process. The mass loss rate also indicated that the PALMS process effectively remove the rough printed features from ALM components to produce a surface finish comparable with conventionally machined CM components. The current density at the beginning (I_a) and the end (I_b) lies in the same range for both CM and ALM samples (Table 3). Although both CM and ALM surfaces were smoothened to a very similar level (Figs. 6 and 7), it was not clear if the changes in current density of the

two materials were directly related to process time or if it was related to the initial surface roughness. The PALMS process in general, at one fixed set of process parameters (temperature, voltage, pH and ion concentration) had shown good repeatability in current density based on the standard deviations from 3 individual experiments (Table 3). The decrease in current density confirmed the process was smoothing rough components [11].

4.3.3 Changes in Mechanical Properties

It is generally recognised that one of the common post-print treatments for ALM components is stress relieving by additional heat treatment [2-5, 15]. Because the EPPo process is reported to reduce surface hardness [18], it is important to establish the effect of the PALMS process on the mechanical properties of the surface and bulk of the treated samples. A change in mechanical properties such as a reduction in surface or bulk hardness may indicate the need for additional, Post-PALMS heat treatment. The surface micro-hardness on both the surface (HV_2) and cross-section ($HV_{0.5}$) were summarised in Table 4. The instrumental indentation hardness depth profile was measured with a 200mN force, from the edge of a cross-sectional test piece (Fig. 8). The Pre-PALMS test results confirmed the AISI 316 specification for both materials were similar, *i.e.* both materials showed surface micro-hardness was higher than their bulk (cross-section) micro-hardness. The effect of printing direction of ALM did not affect the main material mechanical property for this chosen method (Table 4) since the hardness was similar, both on the surface and in cross section, (i.e. at 90 degrees to each other). The hardness of ALM was much higher than in the CM samples, as evidenced by the hardness at the near-surface (Fig. 8). However, it is worth noting that XRD

17

results (Section 4.3.4) indicate a reduction in diffraction peak widths, which could be linked to a near-surface residual stress decrease. Similar evidence has been reported in studies on DMLS austenite and its grain size which led to elevated mechanical properties [4, 20, 23, 24]. Whilst the mechanical properties of both materials did not experience obvious changes in the bulk material structure after the PALMS process (evidenced by cross-sectional $HV_{0.5}$ and $HV_{0.2}$), the outer surfaces were both slightly hardened (HV_2 and $HV_{0.2}$). XRD results show no sign of phase change to correlate to this change in microhardness. We do observe a slight increase in chromium concentration at the surface Post-PALMS (Table 5). Corroborating this result, a very superficial dealloying was shown to occur upon EPPo of another chromium steel [14], with a chromium rich surface layer of approximately 10nm in thickness formed. The surface enrichment in chromium (which is likely to be due to its lower susceptibility to electrodissolution compared to iron) could provide a source of the slight increase in surface hardness observed here. Another possible contribution to the hardness readings could be brought by the stark difference in roughness between Pre- and Post-PALMS surfaces. As the Post-PALMS process measured by OSP ended with $S_z < 8.3$ µm for both CM and ALM cases, the first sampling point of the hardness depth profile was set at the asperity S_z level (about 10 µm) to make sure the reading obtained was representative. Whereas EPPo was reported to start with smooth surfaces (typically $S_a < 1$ µm) and polish them, with associated reductions in surface hardness [18]; in contrast, the PALMS process started with rougher surfaces (typically $S_a \gg 1$ µm) and smoothed them, with associated increases in surface hardness.

4.3.4 Changes in Surface Chemistry and Structures

The CM materials (Wrought reference composition obtained by EDS in Table 5) used in this study showed good agreement with the material specification in the literature (Literature Ref [25]) for a typical AISI 316. (Wrought Ref = the polished, pre-grit blasted CM AISI 316 material). The very small amounts of Al and O in the Wrought Ref material were attributed to the lapping and polishing media used as well as some surface oxidation in the ambient environment. The Pre-PALMS CM results from EDS deviated from the standard material specification due to grit blasting with carbon-contaminated Al_2O_3 that resulted in embedding of oxides and carbon contaminations. Higher amounts of Si for the ALM as printed material surface was attributed to the glass bead blasting typically used after metal printing. The PALMS-process cleaned and reduced the surface contaminations by reducing the level of oxides and carbon which showed a similar beneficial effect to the traditional EPPo process [18]. The surface light oxides after the PALMS process were thought to be mostly at the very top surface such that a sputter cleaning process during a PVD coating cycle would be capable of removing these oxides thereby leading to a similar level of adhesion to the conventionally polished quality of surface. This has been shown to be the case (Table 2). The Literature-Ref [25] chemistry of the surface for AISI 316 was revealed after the PALMS process in general.

An insight into changes in the surface microstructure with PALMS treatment was obtained using XRD (Fig. 9). Austenite diffraction patterns show consistent peak positions both Pre- and Post-PALMS. The observed decrease in peak width after PALMS suggests either a decrease or no changes in residual stress at the interface. Therefore, the increase in surface hardness Post-PALMS is unlikely to be associated with increased residual stress and instead is thought to result from some other

microstructural or composition change. Detailed discussion of XRD will be shown in 4.4.3.

4.3.5 Effect of PALMS Process on the Surface Microstructures

The bulk mechanical and chemical properties were comparable Pre- and Post-PALMS for both CM and ALM. The DMLS printed ALM test discs exhibited great differences in surface microstructure in terms of density and structure compared with the CM discs (Figs. 10a and 10b). This was due to the nature of the DMLS process involving granules fused by multiple thermal cycles, irrespective of material [4]. The CM samples were relatively featureless optically whilst solidification of melted powder droplets was clearly shown in the ALM samples. However, no large scale porosity defects were observed between different layers and powder droplets therefore the material density with this structure would not result in any substantial loss in mechanical properties (Figs. 10c and 10d).

Both the conventional lapped and polished CM and the PALMS smoothed CM surfaces did not show the grain structure clearly at the same length scale (Figs. 11a and 11c) and the lapping marks were evident on the as-polished CM sample (11a) and local pitting was observed in the Post-PALMS CM sample (Fig. 11c). In contrast to the CM samples the ALM structure of the powder droplets and layered structure became much clear after PALMS treatment (Figs. 11b and 11d) and did not exhibit substantial pitting defects compared to the PALMS treated CM surface (Figs. 11c and 11d). The Post-PALMS surface finish of the ALM sample (11f) was clearly superior to that of the CM sample (11e) with the CM sample exhibiting a much higher density of surface pitting for the same PALMS process conditions. The S_z differences were consistent with these

pitting density observations although the same level of S_a and S_q occurred in both CM and ALM samples (Figs. 6 and 7).

The porosity of the surface in terms of pores/pits was quantified in Fig. 12 using OSP and processing software contour filtering to reveal pores with different depths. The number of pores/particles with depth/height greater than 500 nm dominated the PALMS treated CM surface whilst no structured pores were identified on the PALMS treated ALM surface (Figs. 12a and 12b). These OSP results were in good agreement with SEM observations in Fig. 11. The PALMS smoothing process revealed a layered structure in the ALM samples (deeper red lines in Fig. 12b) and progressively reduced the depths of these lines as the process time increased to 90 minutes (Figs. 12b and 12c). The Post-PALMS ALM sample was featureless (improved roughness) when a 500 nm contour filter was applied thus a 200 nm filter was employed. It should be noted that a traditional lapping and polishing process with a highly mirror finished surface would typically lead to an extremely smooth surface in which the depth of pores were typically only visible with filters of 50 nm or lower (Fig. 12d). However, the specification of this study was not to compare the super mirror finished process with PALMS smoothed finishes. The PALMS process proved capable of achieving the specified surface finish as was discussed in previous section (4.3.1). The ALM surface was much smoother with fewer pores/particles after the PALMS treatment. The OSP results further confirmed the SEM observations (Fig. 11) showing that ALM with PALMS treatment exhibited superior surface finish to the CM samples smoothed using the same PALMS process parameters. As tiny amounts of oxides (around 1 wt%) were discovered after the PALMS process (Table 5), an in-depth analysis probing EDS spectra inside and outside

of the pores in Fig. 11c showed greater concentrations of oxides in the bottom of pits than on the smooth surface areas on the CM PALMS treated surface.

A grain structure study showed that a highly polished conventional CM AISI 316 surface featured only machining marks, even at very high magnification using SE mode in the SEM (Fig. 13a) whereas the PALMS treated ALM surface exhibited the finest grain structure with uniform grain size across the surface (Fig. 13d). Such fine grain structures existed in the entire rapidly solidified metal powder droplets (Fig. 10b), with orientation independent of the direction of printing. This grain structure could not be found in the PALMS treated CM surface. The nature of these fine structures is related to the principle of ALM technology involving rapid solidification [4] and the manufacturing route for the feed powder. The PALMS treatment smoothed the surface asperities and maintained theses fine grain size structures without substantial pitting effects compared with the CM samples. Therefore, overall a better surface finish was achieved on the ALM surface after the PALMS process.

4.4 Final Discussion of Key Findings

4.4.1 Process Effectiveness

Conventional EPPo has been widely used for the exceptional mirror finishing quality surfaces with minutes to hours of processing time, or as a mean of cleaning process for the rusty surfaces or de-burring surfaces. The key focus was in the polishing range where roughness started from $S_a < 1$ µm [11, 12]. The rough surface of ALM technology manufactured parts has not yet been studied by EPPo comprehensively. Conventional EPPo focused on the polishing regime and kept the geometrical features of the components that would possibly lead to longer time in treating rough surfaces

with features maintained. The prototype design of PALMS technology considers the principle of EPPo and adds additional design features for floc filtration and condition monitoring. PALMS prototype machine demonstrated a 10 minutes process time was sufficient to get the roughness down up to 80% of its original status (both CM and ALM, Figs. 6 and 7). The surface would possibly undergo the EPPo polishing regime when the roughness S_a was less than 1 µm. The precision of the manufactured surface then depended on the specific surface parameters to be achieved as a function of time. The mechanistic nature of the PALMS process in treating CM and ALM will need to be further investigated in future work, however, it can be concluded that the current PALMS set up is effective in dealing with rough ALM surfaces.

4.4.2 Residual Surface Oxide and Coating Assessments

The initial investigation on the surface of the PALMS processed CM and ALM test discs showed a small amount of oxides existed in the general post-PALMS surfaces. This is consistent with the conventional EPPo process since oxidation is an integral part of the polishing process [11, 12]. The residual oxides on the PALMS/EPPo processes could restrict the direct use of the treated surfaces in certain applications *e.g.* with post-smoothing coatings, regardless of the amount of oxides on the surface. It was found that the level of residual oxide on the PALMS treated surface matched the level on the CM lapped surface, *i.e.* specific additional surface preparations may not be needed for post-PALMS components (Table 5). This was confirmed by the assessments of the PALMS treated surfaces with additional PVD coatings deposited (both CM lapped and PALMS treated). The coating adhesion level showed equivalence to the conventionally polished and lapped surface. It seems likely that the sputter cleaning stage of the PVD coating

processes removed the thin oxide layers from both CM and ALM PALMS-smoothed surfaces prior to coating deposition. The improvements in friction and wear results seem most likely attributed to the nature of the post-PALMS textured surface, dimpled with reduced contact asperities. As blasting is one of the most commonly used methods for the post-printing components in ALM industry, PALMS brings additional benefits by additional surface cleaning, *i.e.* reducing the SiO_2 (Table 5) associated with glass beads blasting.

4.4.3 Roughness, Hardness, Residual Stress, XRD

In the polishing regime of the conventional EPPo process, the surface mechanical hardness of CM samples was generally considered to be reduced along with reduction in the surface residual stress in line with the reduction in roughness [18]. Rough surfaces (S_a > 2 µm, S_z > 20 µm) smoothed by the PALMS process, however, show evidence of a slightly hardened layer within the very top surface. The PALMS process did not compromise the bulk properties of both CM and ALM samples (Fig. 8 and Table 4) whereas the very top surface layers were hardened (Table 4). It was also co-evidenced by Rockwell C evaluation of the PVD coated sample described in Table 2 for adhesion analyses, *i.e.* a hardness value was measurable on PALMS treated and coated surfaces with 150 kgf load applied whereas it was impossible to get a hardness reading at the same load due to lack of load support for a CM AISI 316 lapped and polished samples with the same coatings.

Further work is required to identify the cause of surface hardening in the PALMS treated samples. This observation is in contrast to that reported for EPPo [18]. The high Pre-PALMS roughness itself might explain the lower microhardness. Alternatively from

a surface chemistry point of view, a slightly higher chromium content was observed post-PALMS in both CM and ALM samples (Table 5,) a result confirming independent GDOES observations [14]. This altered superficial composition could also be associated with accumulation of hard carbide inclusions that are less prone to anodic dissolution. X ray diffraction (XRD) reveals a pattern identified with austenite, or γ-phase of iron, as is expected of AISI 316 stainless steel. The peaks observed Post-PALMS are consistently narrower compared to their Pre-PALMS counterparts, by a factor 2 (Fig. 9b), both in Bulk and ALM samples, and both on up- and downskin surfaces in the case of ALM. The reduction in surface roughness could contribute to a reduction in XRD peak widths due to lower scattering. Another possible contribution for XRD peak narrowing is lower residual stress in the newly exposed surface microdomains. Since the machining and subsequent sandblasting used to make the CM samples are expected to produce surfaces with significant residual strain, their removal through PALMS would indeed result in a reduction in observed residual strain. Likewise for ALM samples, the rapid local heating and cooling linked to the sintering of metal powder particles is expected to produce a superficial layer of significant residual strain. The consistent and significant reduction in diffraction peak widths, if confirmed to be caused by a reduction in residual stress, would suggest a potential for better resistance to superficial fatigue crack initiation and subsequent damage, which remains to be investigated but could represent a crucial advantage for the adoption of ALM in more demanding applications.

Another robust outcome in the XRD results is a redistribution in the relative peak intensities. The evolution of these ratios means that different planes in austenite's face centred cubic (fcc) crystallographic lattice are preferentially aligned with the surface. When observed in comparing Post-PALMS to Pre-PALMS samples, this redistribution

could therefore be the mark of a selective electrodissolution of microdomains based on which crystallographic plane is exposed to the electrolyte during the process itself. The change induced by the process, while consistently reproducible for each type of machining, diverges between CM and ALM surfaces. For example, the 2 2 0 Post-PALMS peak is underrepresented on CM samples (Fig. 9a), but overrepresented in ALM ones. This divergence renders definitive conclusions on selective electrodissolution difficult to make with the body of data collected, yet underlines the potential in taking this type of investigation further. Peak analysis revealed no further significant effect of PALMS. In particular no shift in peak position, which could be linked to changes in interplanar spacing in the lattice, *e.g.* in some cases of dealloying, was observed.

Different ALM methods are reported to produce different mixes of austenite and martensite phases [23, 24, 26]. The main structure of the ALM AISI 316 test pieces in the present study shows the austenite features have been maintained during the PALMS smoothing. Thus DMLS printed ALM test samples studied in this case exhibited the same major phases as the CM AISI 316, *i.e.* austenite characteristics were maintained as were originally printed. Therefore the increase in surface hardness observed following the PALMS process must be due to microstructure changes.

4.4.4 Pitting Analyses

Pitting occurred at different size scale and quantity following the PALMS process compared with the traditional lapped and polished CM surfaces (Fig. 11). In the anodic hydrolysis process at high voltage, the coverage and origin of oxides clusters on the surface asperities were thought to be selective, based on the electric potential

distribution on the rough surfaces. The surface oxide clusters had been removed continuously during the electrical discharge such that the surfaces were smoothed with the oxides peaks being removed. There existed a lot more local pitting of a larger scale on the CM surfaces compared with ALM surfaces which was postulated to be caused by either the local electrical discharge of the oxides generated, or localised 'attack' of chromium carbide grains that acted as electrical insulators, or a combination of the two. The former would be related to the PALMS anodic process whereas the latter are commonly seen in stainless steel alloy structures as regular round shaped grains [27].

Further investigation by EDS of the pits shown in Figs. 11 and 13 suggested that most of the residual oxide were located inside these pitting areas whereas the flat top surfaces were oxygen free after the PALMS process. For the electrochemical gas discharge, the oxides on the peak positions of the surface would be more readily removed by PALMS than the pits at the trough positions. Therefore, the post-PALMS surface finish was largely improved within a 10 minute process by continuous removal of oxides at the peak positions (both CM and ALM) whilst tiny amounts of residual oxides were left in the troughs / pits.

The PALMS treated CM surface exhibited more pitting areas than the ALM one, even though both had similar surface roughness prior to the PALMS treatments. The OSP and SEM at higher magnification indicated that the grain size and structural distribution, as well as the printing paths, could affect the surface not only in mechanical properties, but also structural and electrical potential variation at some localised points (Figs. 12 and 13). The toughs in the ALM samples are of a morphology which reflects layered and granular nature of the ALM process, *i.e.* linear troughs and skeletal troughs are observed (Figs 12 and 13). The PALMS process reveals the linear and skeletal gaps of

the droplets/layers of the smoothed ALM surface; whereas the process created large scale pits on the otherwise homogeneous CM surface. One hypothesis is that the pit morphology observed in the CM material and absent in the ALM material could be related to the presence of chrome carbide grains in CM and corresponding absence in the ALM samples. Further work is required to identify the cause of the pitting.

5. Conclusions

The PALMS technology, derived from electrolytic plasma polishing, was developed and the results of its application on Additive-Layered Manufactured pieces are presented in this article. A contactless method largely independent from geometry and relying on environmentally friendly electrolytes, PALMS represents a versatile finishing method for ALM. A 5-fold smoothing of rough ALM surfaces was demonstrated here, within 10 minutes of processing and without adverse effect on other surface properties, confirming significant potential of this method for metal AM industrial application. The degree of smoothing could be further improved and tailored by varying processing time. XRD demonstrated a drastic reduction in diffraction peak widths, which could be linked to lower residual stress, in similar proportions for both ALM and CM samples, suggesting a potential for better resistance to mechanical and fatigue damage of Post-PALMS pieces. PVD coatings were applied post PALMS to demonstrate compatibility with further surface treatments. Future work will investigate PALMS treatment of complex geometries allowed by ALM.

Acknowledgements

References

1.   Ford, S. and M. Despeisse, *Additive manufacturing and sustainability: an exploratory study of the advantages and challenges.* Journal of Cleaner Production, 2016. **137**: p. 1573-1587.
2.   Frazier, W.E., *Metal Additive Manufacturing: A Review.* Journal of Materials Engineering and Performance, 2014. **23**(6): p. 1917-1928.
3.   Guo, N. and M.C. Leu, *Additive manufacturing: technology, applications and research needs.* Frontiers of Mechanical Engineering, 2013. **8**(3): p. 215-243.
4.   Herzog, D., et al., *Additive manufacturing of metals.* Acta Materialia, 2016. **117**: p. 371-392.
5.   Lewandowski, J.J. and M. Seifi, *Metal Additive Manufacturing: A Review of Mechanical Properties.* Annual Review of Materials Research, 2016. **46**(1): p. 151-186.
6.   Pinkerton, A.J., *[INVITED] Lasers in additive manufacturing.* Optics & Laser Technology, 2016. **78**: p. 25-32.
7.   Thompson, M.K., et al., *Design for Additive Manufacturing: Trends, opportunities, considerations, and constraints.* CIRP Annals - Manufacturing Technology, 2016. **65**(2): p. 737-760.

8. Cordero, Z.C., et al., *Powder bed charging during electron-beam additive manufacturing.* Acta Materialia, 2017. **124**: p. 437-445.

9. Murr, L.E., et al., *Metal Fabrication by Additive Manufacturing Using Laser and Electron Beam Melting Technologies.* Journal of Materials Science & Technology, 2012. **28**(1): p. 1-14.

10. Kellogg, H.H., *Anode Effect in Aqueous Electrolysis.* Journal of The Electrochemical Society, 1950. **97**(4): p. 133-142.

11. Nestler, K., et al., *Plasma Electrolytic Polishing – An Overview of Applied Technologies and Current Challenges to Extend the Polishable Material Range.* Procedia CIRP, 2016. **42**: p. 503-507.

12. Parfenov, E.V., et al., *Towards smart electrolytic plasma technologies: An overview of methodological approaches to process modelling.* Surface and Coatings Technology, 2015. **269**: p. 2-22.

13. Yerokhin, A.L., et al., *Plasma electrolysis for surface engineering.* Surface and Coatings Technology, 1999. **122**(2): p. 73-93.

14. Yerokhin, A., et al., *Charge transfer mechanisms underlying Contact Glow Discharge Electrolysis.* Electrochimica Acta, 2019. **312**: p. 441-456.

15. Kumbhar, N.N. and A.V. Mulay, *Post Processing Methods used to Improve Surface Finish of Products which are Manufactured by Additive Manufacturing Technologies: A Review.* Journal of The Institution of Engineers (India): Series C, 2016.

16. Dehoff, R.R., F.A. List III, and K. Carver, *Evaluation Of Electrochemical Machining Technology For Surface Improvements In Additive Manufactured Components.* 2015, Oak Ridge National Laboratory (ORNL), Oak Ridge, TN (United States). Manufacturing Demonstration Facility (MDF).

17. McGeough, J.A., *Principles of electrochemical machining.* 1974: CRC Press.

18. Yerokhin, A., A. Pilkington, and A. Matthews, *Pulse current plasma assisted electrolytic cleaning of AISI 4340 steel.* Journal of Materials Processing Technology, 2010. **210**(1): p. 54-63.

19. Vogt, H., *Contribution to the interpretation of the anode effect.* Electrochimica Acta, 1997. **42**(17): p. 2695-2705.

20. Mower, T.M. and M.J. Long, *Mechanical behavior of additive manufactured, powder-bed laser-fused materials.* Materials Science and Engineering: A, 2016. **651**: p. 198-213.

21. S.A.S., A., *WC-C:H coating by Physical Vapour Deposition*, in *Airbus Process Specification*. 2010, AIRBUS S.A.S. ENGINEERING DIRECTORATE: BLAGNAC Cedex, France. p. 16.

22. Yang, L., et al., *Friction reduction mechanisms in boundary lubricated W-doped DLC coatings.* Tribology International, 2014. **70**: p. 26-33.

23. Gu, D. and Y. Shen, *Processing conditions and microstructural features of porous 316L stainless steel components by DMLS.* Applied Surface Science, 2008. **255**(5): p. 1880-1887.

24. Coffy, K., *Microstructure and Chemistry Evaluation of Direct Metal Laser Sintered 15-5 PH Stainless Steel.* 2014.

25. Klar, E. and P.K. Samal, *Powder Metallurgy Stainless Steels: Processing, Microstructures, and Properties.* 2007: ASM International.

26. Zhang, Y., et al., *Characterization of laser direct deposited metallic parts.* Journal of Materials Processing Technology, 2003. **142**(2): p. 582-585.

27.   Mills, K. and A.I.H. Committee, *ASM Handbook. Volume 9. Metallography and Microstructures*. 1985: ASM International.
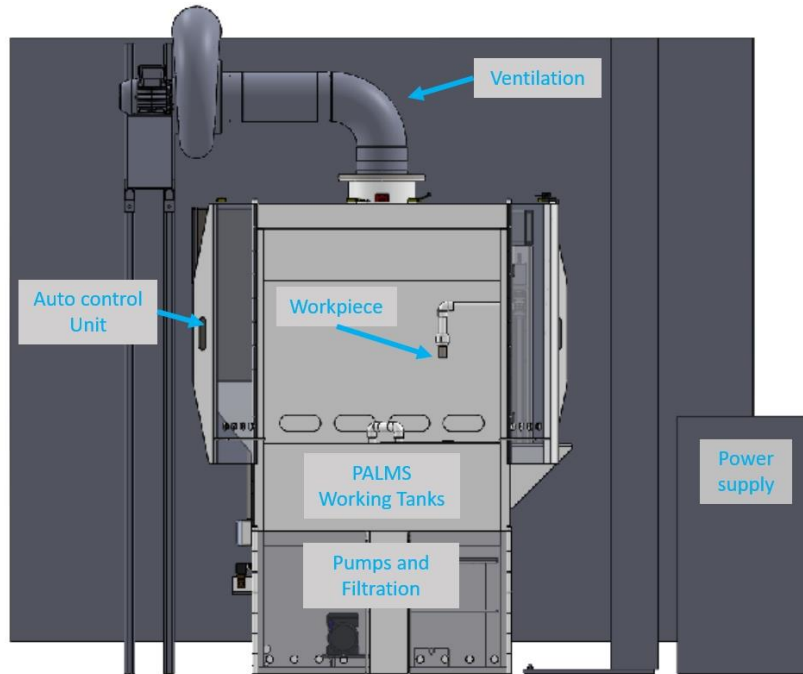
Figure Captions

Fig. 1. PALMS Industrial Prototype Machine Configuration for Additive Manufactured Components
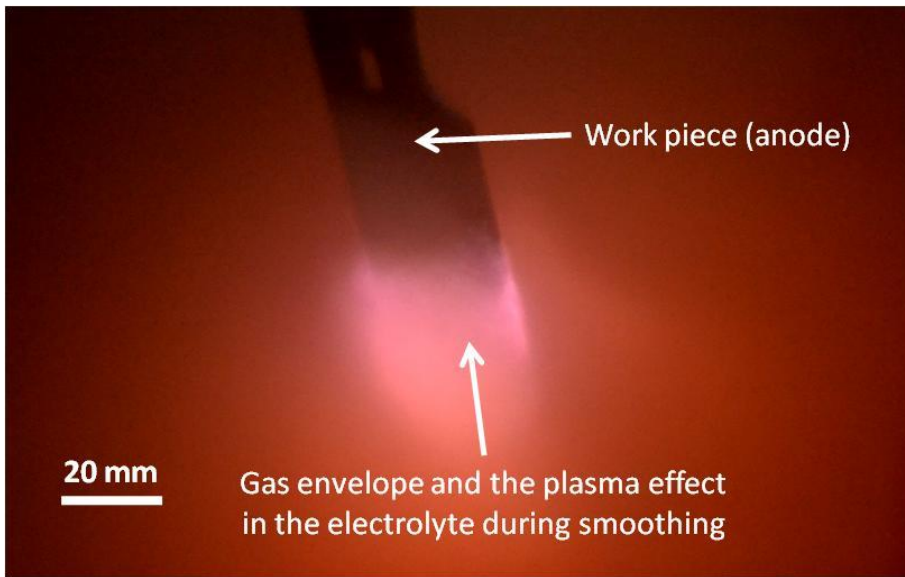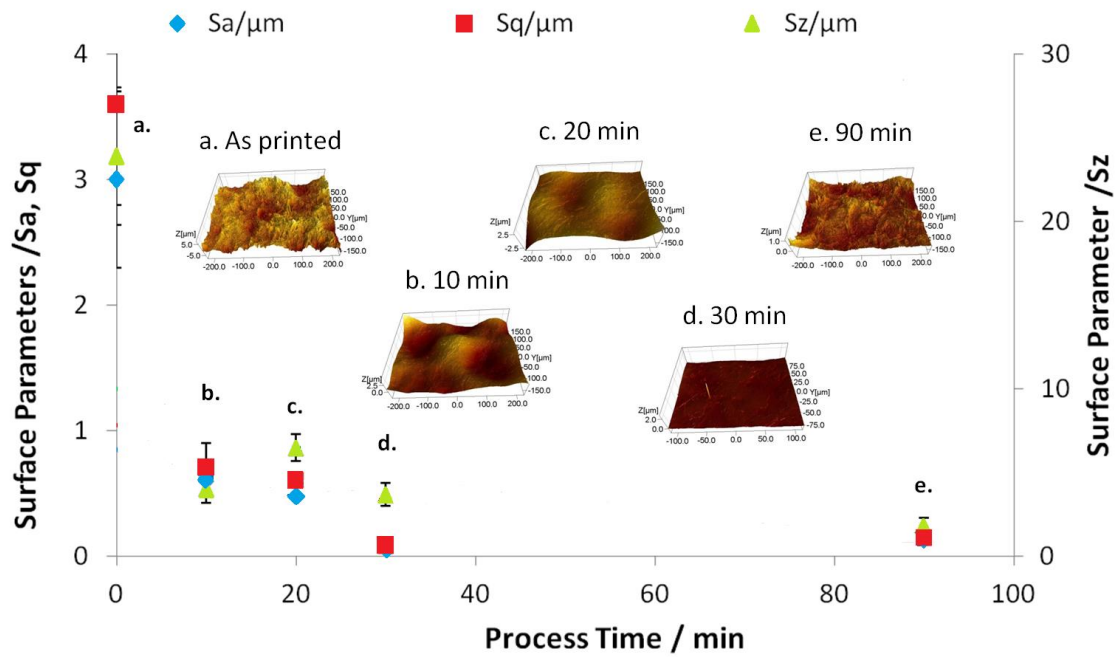

Fig. 2. A Work Piece Example of PALMS Process

Fig. 3. Controlled Surface Parameters of ALM Printed AISI 316 Discs vs. Treatment Time
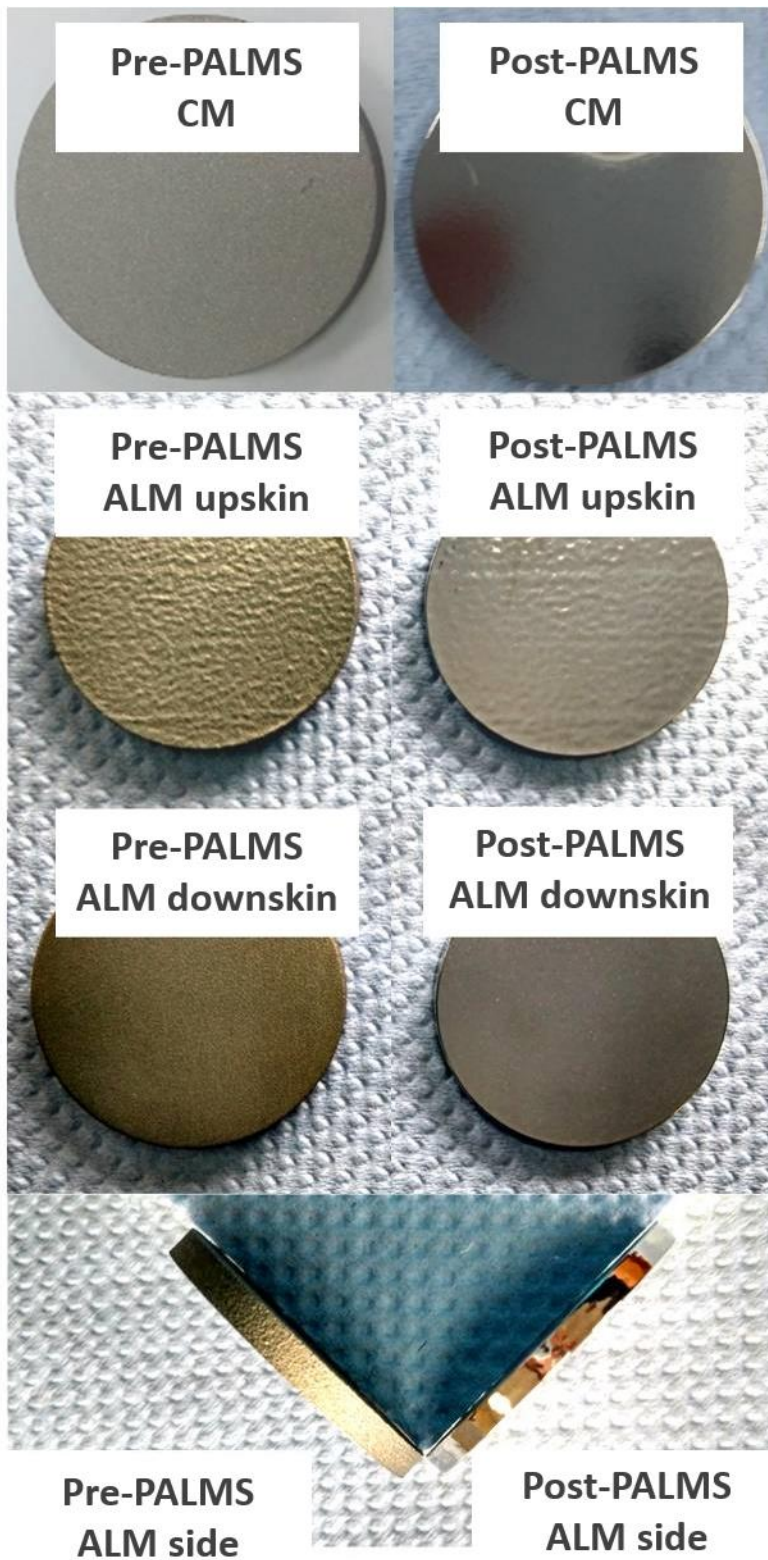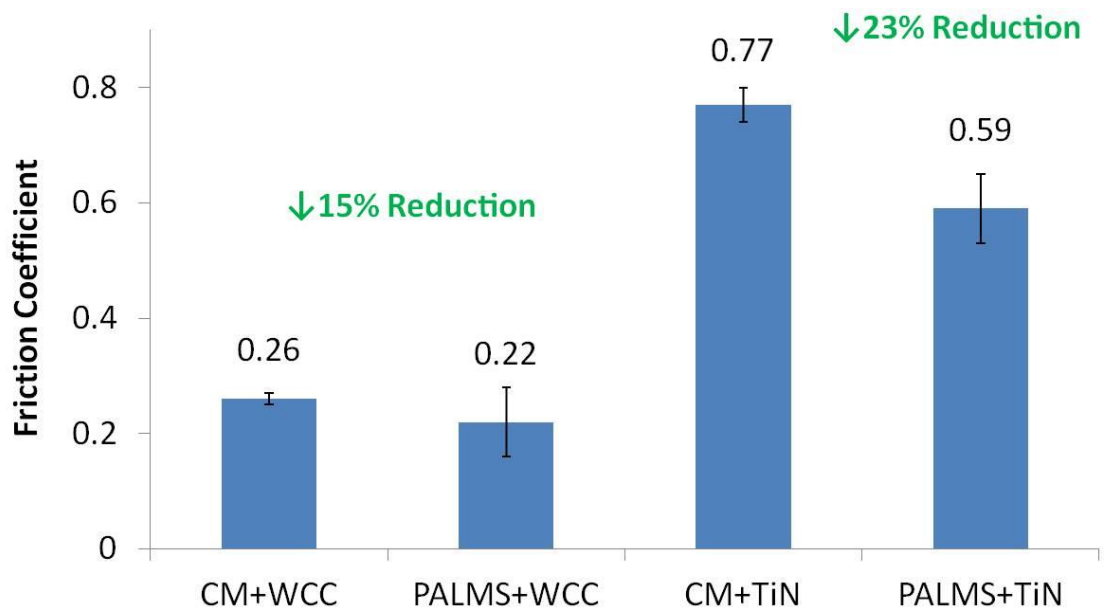

Fig. 4. Optical Inspections of PALMS Treated CM and ALM AISI 316 in 10min

Fig. 5. Average Friction Coefficient of coated CM samples with/without prior PALMS treatment
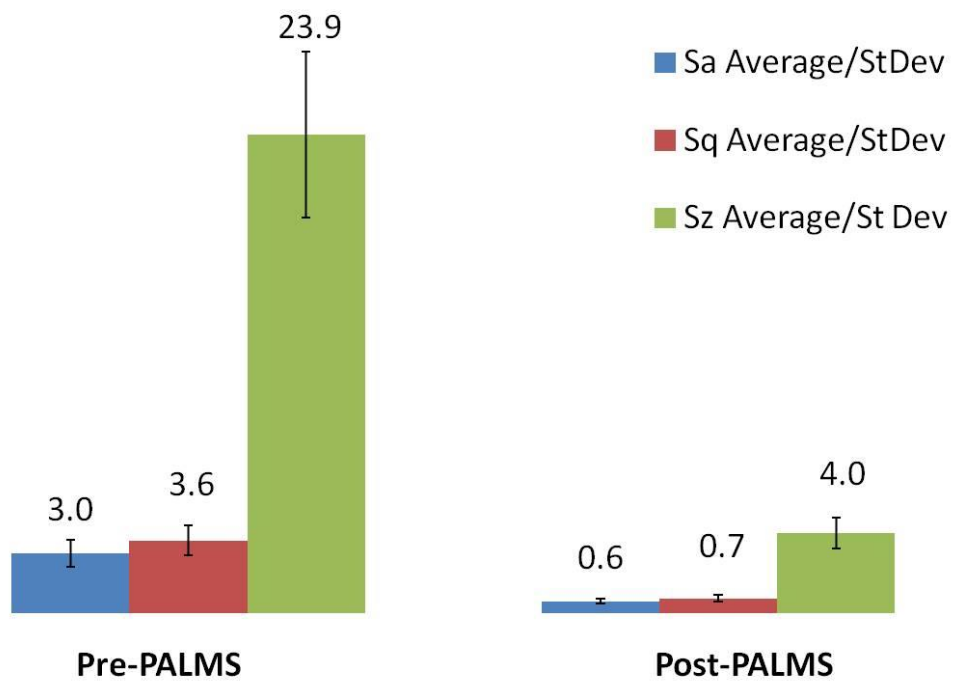

Fig. 6. CM AISI 316 Roughness Pre- and Post- PALMS
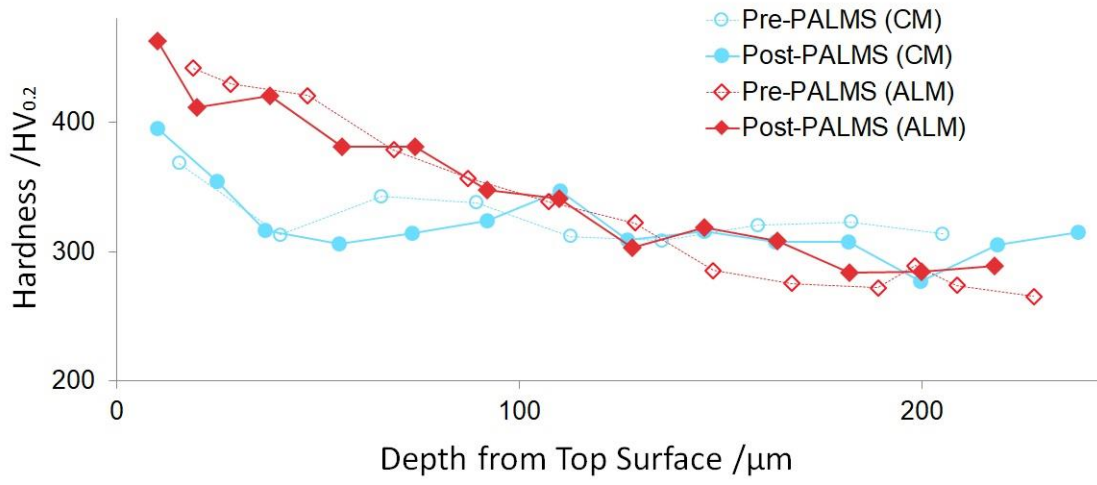

Fig. 7. ALM AISI 316 Roughness Pre- and Post- PALMS


Fig. 8. Nano-indentation Cross-section Depth Profile on Post-PALMS AISI 316 Samples (left) and Indentation Marks Distribution (right)

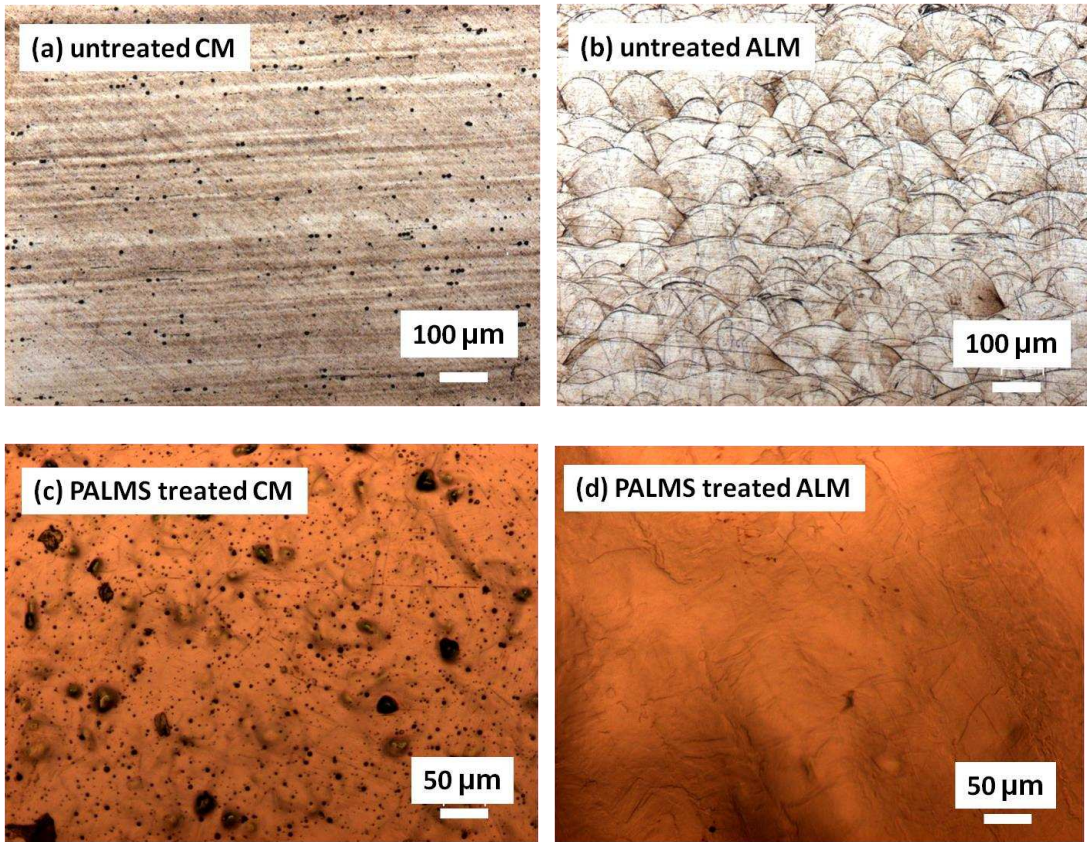Fig. 9. XRD of Both Pre- and Post-PALMS Samples

Fig. 10. Optical Cross-sectional (top) and Topographic (bottom) Comparisons of the Macro Scale Structure of CM and ALM AISI 316

Fig. 11. SEM Topography Assessment on the Conventional Polished CM AISI 316 Pre- and Post-PALMS

Fig. 12. OSP Porosity and Pore Quantification

Fig. 13. Morphological Study on the AISI 316 Grain Structure Pre- and Post-PALMS

Table Captions

Table 1 Comparison of PALMS with State of the Art Methods

Table 2 Coated Surface Assessments of PALMS treated and lapped/polished AISI 316

Table 3 Mass Loss and Change in Current Density Related to Sample Geometry in a 10 min Treatment

Table 4 Effect of PALMS on the Mechanical Properties of CM and ALM

Table 5 The Change in Surface Chemistry of the PALMS Process

Fig. 1. PALMS Industrial Prototype Machine Configuration for Additive Manufactured Components

Fig. 2. A Work Piece Example of PALMS Process

Fig. 3. Controlled Surface Parameters of ALM printed AISI 316 discs vs. Treatment Time

Fig. 4. Optical Inspections of PALMS Treated CM and ALM AISI 316 in 10min (Downskin refers the side lying against the printer bed which is smoother)

Fig. 5. Average Friction Coefficient of coated CM samples with/without prior PALMS treatment
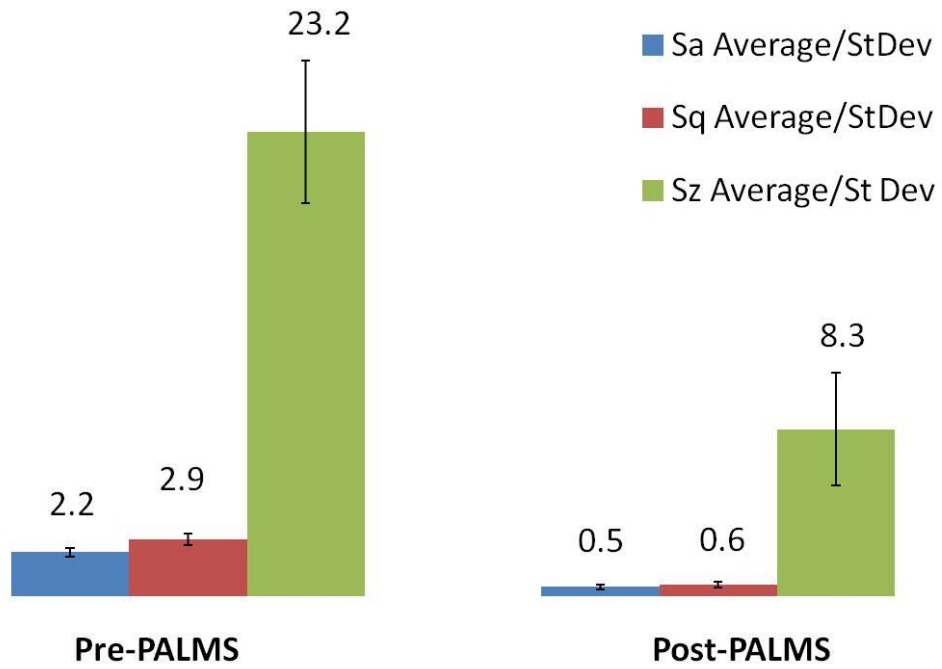
Fig. 6. CM AISI 316 Roughness in μm Pre- and Post- PALMS

Fig. 7. ALM AISI 316 Roughness in μm Pre- and Post- PALMS

Fig. 8. Nano-indentation Cross-section Depth Profile on Post-PALMS AISI 316 Samples (left) and Indentation Marks Distribution (right)
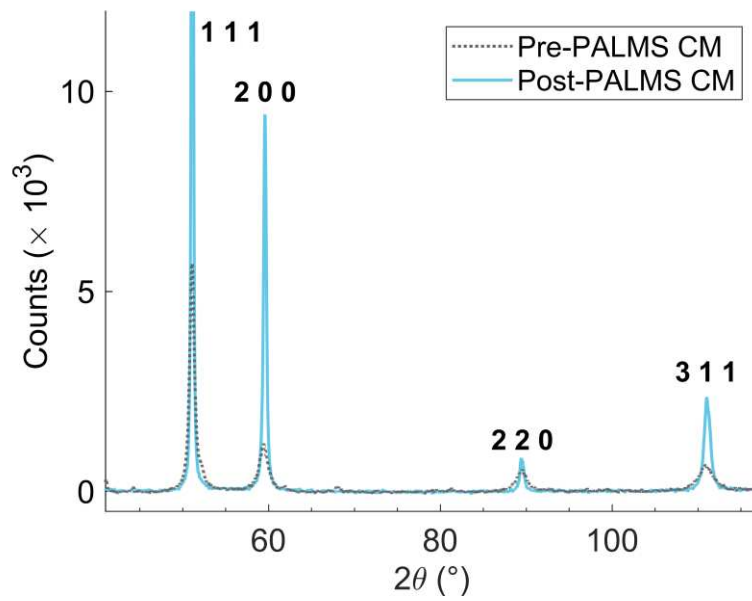
(a) Partial Diffractograms of CM Surfaces Pre- and Post-PALMS, with the Miller

Indices of the Corresponding Austenite fcc Crystallographic Planes
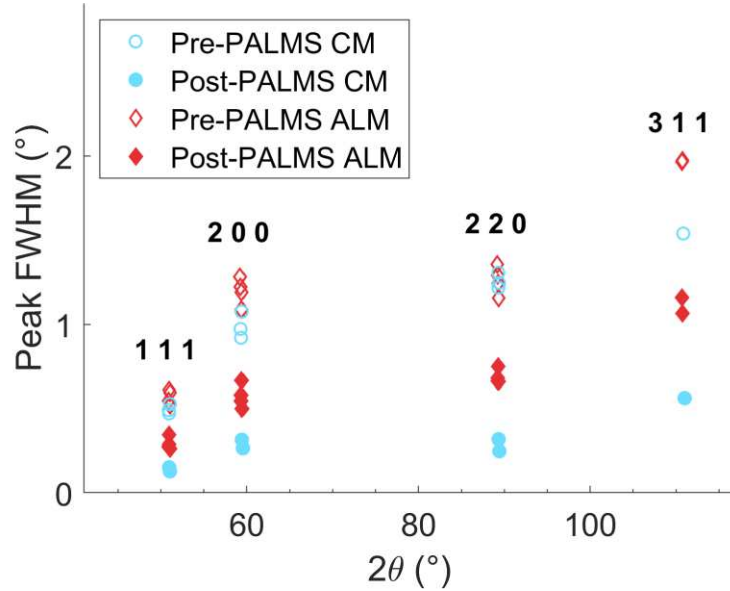
(b) Full Width at Half Maximum, Expressed in 2θ Angles, of All Observed Diffraction

Peaks

Fig. 9. XRD of Pre- and Post-PALMS Samples

Fig. 10. Optical Cross-sectional(top) and Topographic (bottom) Comparisons of the Macro Scale Structure of CM and ALM AISI 316
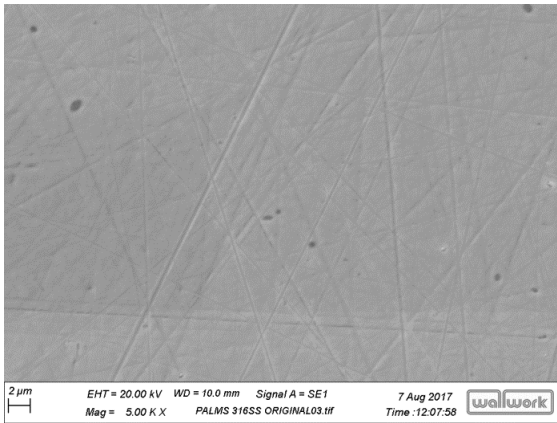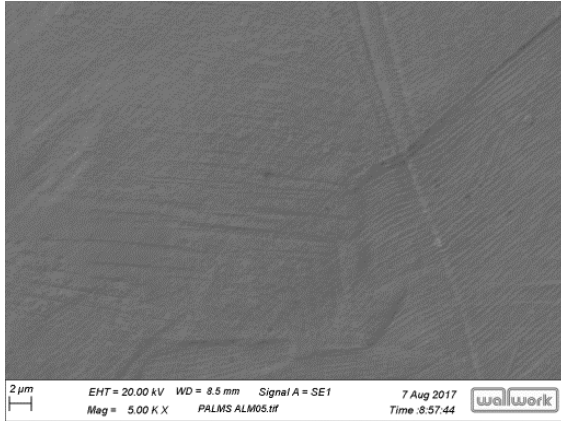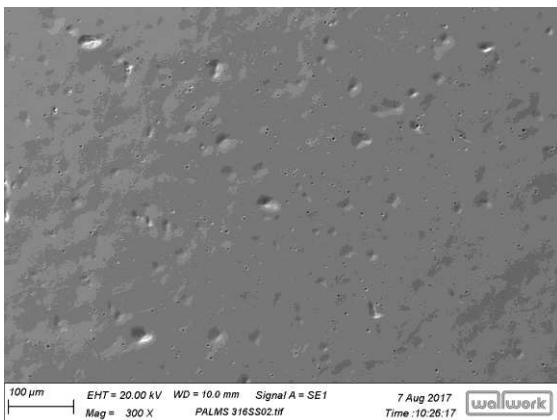
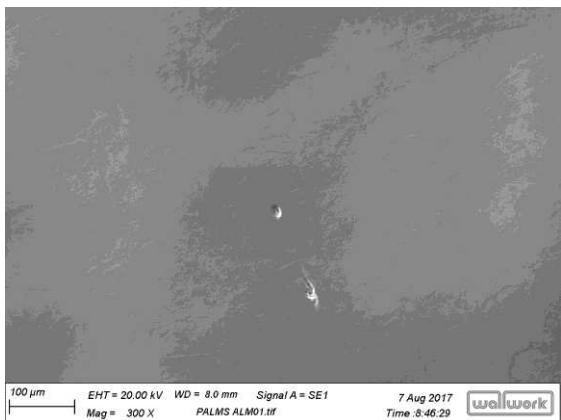(a) Conventional lapped and polished CM
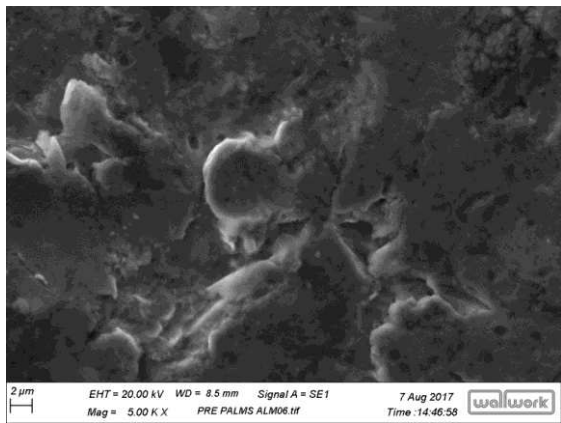
(b) Pre-PALMS ALM
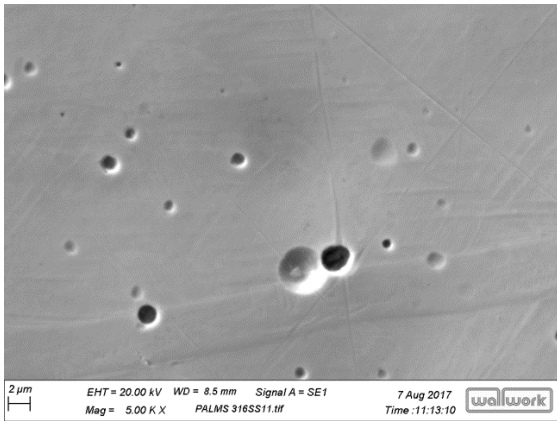
(c) Post-PALMS CM

(d) Post-PALMS ALM

(e) Post-PALMS CM (1)

(f) Post-PALMS ALM (2)

Fig. 11. SEM Topography Assessment on the Conventional Polishing AISI 316 Pre-and Post-PALMS
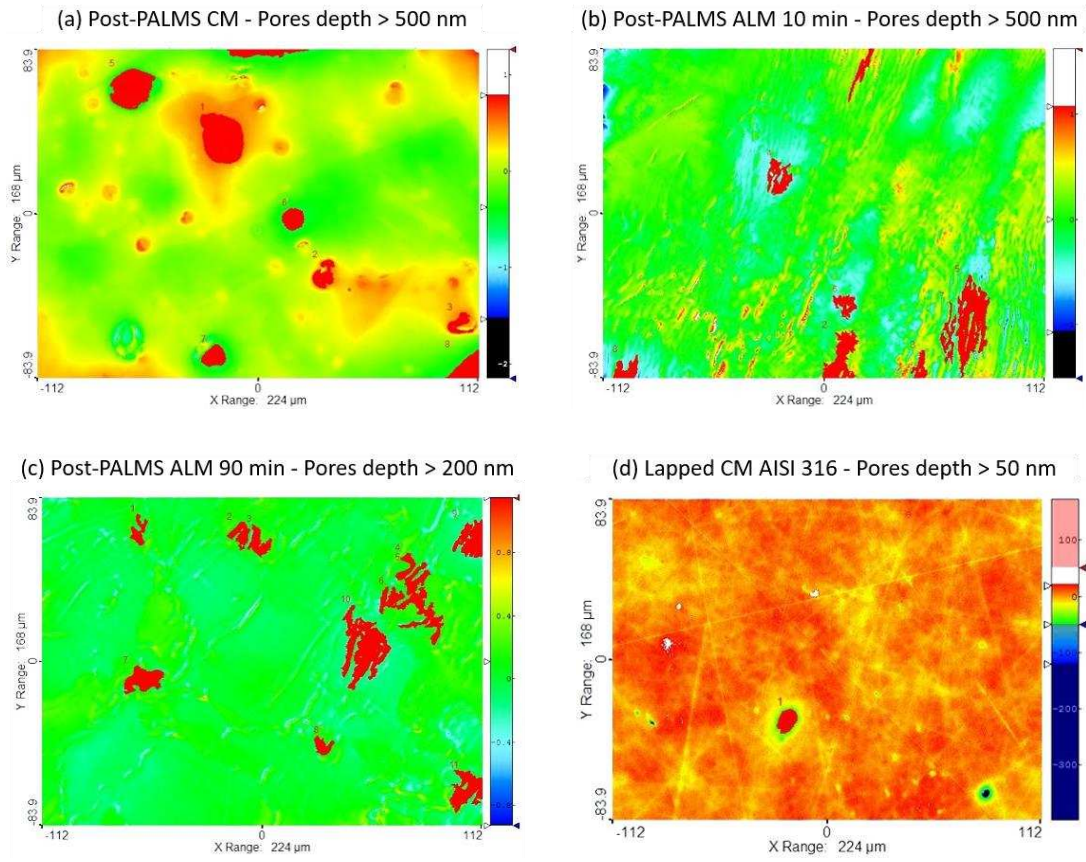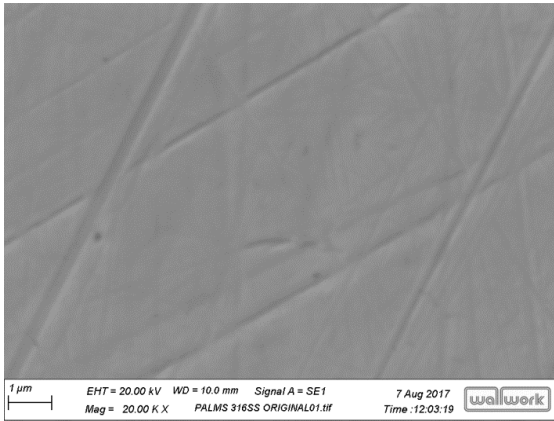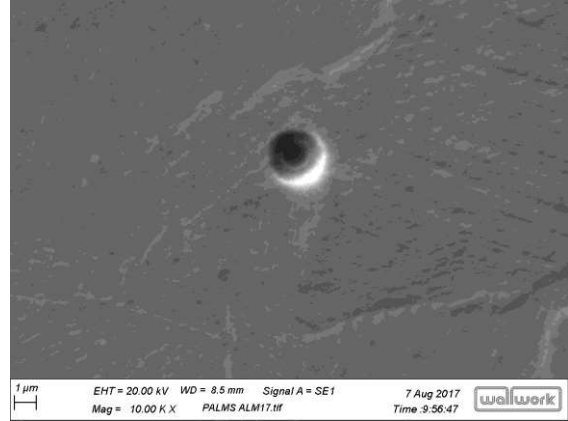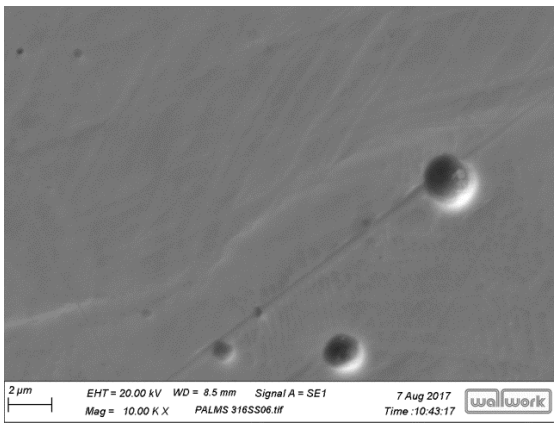
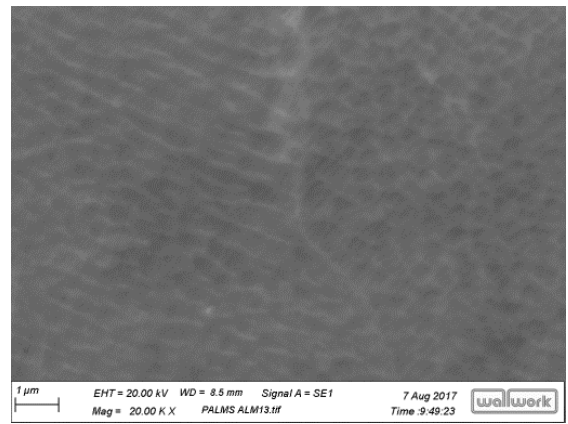**Fig. 12.** OSP Porosity and Pore Quantification

(a) Conventional Polishing CM   (b) Post-PALMS ALM (1)

(c) Post-PALMS CM   (d) Post-PALMS ALM (2) dendritic

Fig. 13. Morphological Study on the AISI 316 Grain Structure Pre- and Post-PALMS

Table 1

Comparison the Pros and Cons of PALMS with the other State of the Art Methods

(Typical process parameters selected as examples)

Techniques for macro finishing	Material removal rate (µm/min)	Energy consumption / Overall cost	Environmental impact	Uniformity	Treating major AM metals*	Can treat roughness range 0.1-50µm
ECM	Average 1	Medium/High	Acidic/Hazardous	Yes	Limited	Yes
MMP	Low	Low/low	Low impact	Yes	Yes	No
Laser Radiation	1.5-30	High/high	Radiation control	No	No	No
Abrasives	Low	Medium/High	Low impact	Yes	No	No
PALMS/EPPo	0.5-5	Medium/Low	low impact	Yes	Yes	Yes

* Titanium, titanium alloys, steel, gold, silver, nickel alloys, copper alloys, aluminum alloys, magnesium alloys.

Table 2
Coated Surface Assessments of PALMS treated and lapped/polished AISI 316

Sample ID	Rockwell C Indentation	Scratch Lc2 /N	Wear Coefficient /μm^3/(m*N)	Max Depth of Wear Scar /μm	Average Surface Roughness S_a /μm
CM+WCC	HF2	10.0±0.3	6200	1.2	0.1
PALMS+WCC	HF2	16.1±3.0	4132	0.5	0.6
CM+TiN	HF2	24.7±1.9	15590	1.2	0.1
PALMS+TiN	HF2	22.2±1.6	1849	0.8	0.6

Table 3

Mass Loss and Change in Current Density Related to Sample Geometry in a 10 min

Treatment

Sample Discs	Gravimetric /%	Material Removal Rate (MRR)/(μm/min)*	Initial Current Density I_a /(A/cm^2)	Final Current Density I_b /(A/cm^2)
CM/Mean	-1.1	1.31	0.43	0.34
CM/StDev	±0.5	±0.08	±0.08	±0.05
ALM/Mean	-1.5	1.91	0.42	0.33
ALM/StDev	±0.3	±0.38	±0.10	±0.02

* Assuming a 7.870g/cm^3 for both CM and ALM AISI 316

Table 4

Effect of PALMS on the Mechanical Properties of CM and ALM

	Micro-hardness Surface / HV_2	Micro-hardness Cross-section / $HV_{0.5}$
CM Lapping/Polishing	250.0±9.1	243.1±10.4
Pre-PALMS /CM	257.7±4.2	242.1±11.6
Post-PALMS /CM	277.7±7.3	234.6±11.1
Pre-PALMS /ALM	301.9±20.3	233.1±10.5
Post-PALMS /ALM	341.4±15.4	247.0±5.7

Table 5
Changes in Surface Chemistry characterised by EDS

wt%	C	Mn	P	S	Si	Cr	Ni	Mo	N	Fe	O	Al
Literature Ref	0.08	2	0.045	0.03	0.75	16-18	10-14	2-3	0.1	62-69	-	-
Wrought Ref[*]	1.01	1.63	0	0	0.24	16.24	9.53	1.44	0.84	67.72	1.35	0.01
Pre-PALMS (CM)[**]	6.59	1.37	0	0.18	0.13	13.66	6.64	0.46	1.37	50.94	8.08	10.6
Post-PALMS (CM)	1.43	1.41	0.10	0	0.34	16.44	9.77	1.65	1.00	66.69	1.10	0.07
Pre-PALMS (ALM)	2.24	1.30	0.80	0	1.81	16.04	10.24	1.45	0.76	58.43	6.63	0.30
Post-PALMS (ALM)	1.74	1.31	0	0.22	0.43	17.58	11.49	1.23	0.78	64.10	1.13	0.00

*CM AISI 316 material used in this study; **Mechanically roughened by grit basting (Al_2O_3)